NANO LETTERS

2007
Vol. 7, No. 9
2835−2842

Organically Modified Silica Nanoparticles with Covalently Incorporated Photosensitizer for Photodynamic Therapy of Cancer

Tymish Y. Ohulchanskyy,[†] Indrajit Roy,[†] Lalit N. Goswami,[†,‡] Yihui Chen,[‡] Earl J. Bergey,[†] Ravindra K. Pandey,[*,†,‡] Allan R. Oseroff,[*,‡] and Paras N. Prasad[*,†]

Institute of Lasers, Photonics and Biophotonics, Department of Chemistry, State University of New York, Buffalo, New York, and PDT Center, Cell Stress Biology, Roswell Park Cancer Institute, Buffalo, New York

Received June 19, 2007; Revised Manuscript Received August 9, 2007

ABSTRACT

We report a novel nanoformulation of a photosensitizer (PS), for photodynamic therapy (PDT) of cancer, where the PS molecules are covalently incorporated into organically modified silica (ORMOSIL) nanoparticles. We found that the covalently incorporated PS molecules retained their spectroscopic and functional properties and could robustly generate cytotoxic singlet oxygen molecules upon photoirradiation. The synthesized nanoparticles are of ultralow size (~20 nm) and are highly monodispersed and stable in aqueous suspension. The advantage offered by this covalently linked nanofabrication is that the drug is not released during systemic circulation, which is often a problem with physical encapsulation. These nanoparticles are also avidly uptaken by tumor cells *in vitro* and demonstrate phototoxic action, thereby highlighting their potential in diagnosis and PDT of cancer.

Introduction. Photodynamic therapy (PDT) is based on the concept that certain therapeutic molecules called photosensitizers (PS) can be preferentially localized in malignant tissues, and when these PSs are activated with appropriate wavelength of light, they pass on their excess energy to surrounding molecular oxygen, resulting in the generation of reactive oxygen species (ROS), such as free radicals and singlet oxygen ($^1O_2$), which are toxic to cells and tissues.[1] PDT is a noninvasive treatment and used for several types of cancers, and its advantage lies in the inherent dual selectivity. First, selectivity is achieved by a preferential localization of the photosensitizer in target tissue (e.g., cancer), and second, the photoirradiation and subsequent photodynamic action can be limited to a specific area of interest. Because the PS is nontoxic without light exposure, only the irradiated areas will be affected, even if the PS does infiltrate normal tissues. Selectivity can be further enhanced by combining the PS with molecular delivery systems and/or by conjugating PS's with targeting agents such as an integrin antagonist or carbohydrates, which have high affinity for target tissue (mainly cancer).[2]

Although PDT is emerging as a choice of treatment for many cancer patients, because of the hydrophobic nature of the most of the PS's, the search is still on for developing an ideal photosensitizer formulation that can be easily injectable in vivo. Numerous approaches have been proposed to achieve not only stable aqueous dispersion but also site-specific and time-controlled delivery of therapeutic agents, often using a biocompatible delivery vehicle.[3] Colloidal carriers for photosensitizers, such as oil dispersions, liposomes, low-density lipoproteins, polymeric micelles, and nanoparticles, are common examples of delivery shuttles for PS molecules.[4−7] They offer benefits from rendering aqueous stability and appropriate size for passive targeting to tumor tissues by the "enhanced permeability and retention" (EPR) effect,[8] and a possibility of bioconjugation approaches to enhance bioavailability as well as tumor targeting.[9] However, the premature release of the PS molecules from carrier vehicles while in systemic circulation results in reduced efficacy of treatment. Because in PDT the release of the PS drugs is not a prerequisite for their therapeutic action (unlike in conventional chemotherapy), covalently incorporating the PS molecules within the delivery vehicles is expected to

* Corresponding authors. E-mail: ravindra.pandey@roswellpark.org (R.K.P.); Allan.Oseroff@RoswellPark.org (A.R.O.); pnprasad@buffalo.edu (P.N.P.).

[†] Institute of Lasers, Photonics and Biophotonics, Department of Chemistry, State University of New York.

[‡] PDT Center, Cell Stress Biology, Roswell Park Cancer Institute.

10.1021/nl0714637 CCC: $37.00
Published on Web 08/25/2007

Scheme 1. Synthesis of the Precursor 3-Iodobenzylpyro-silane (IPS)

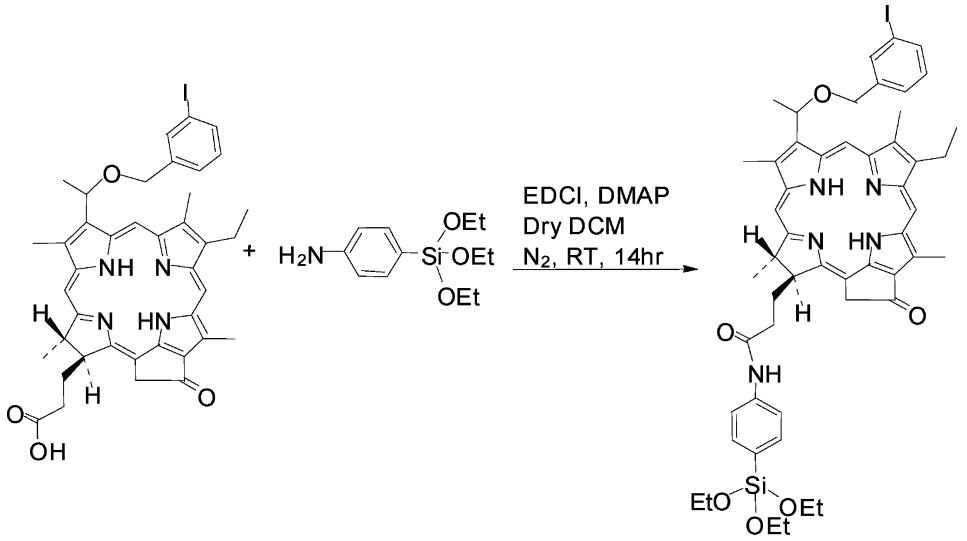

Compound **I** Compound **II**

overcome the drawback of their premature release and thus enhance the outcome of PDT.[10]

In our laboratory, we have developed a highly stable aqueous formulation of organically modified silica (ORMOSIL) nanoparticles encapsulating the hydrophobic PS HPPH [2-devinyl-2-(1-hexyloxyethyl)pyropheophorbide], where the encapsulated PS is able to generate singlet oxygen upon photoactivation owing to the free diffusion of molecular oxygen across the ORMOSIL matrix.[11] However, because of mesoporosity of the ORMOSIL matrix, encapsulation of PS does not exclude the PS release, at least partially, during systemic circulation. To circumvent this problem, here we report a new formulation of the nanoparticles with the PS molecule being covalently linked, instead of just being physically encapsulated. In the first step, we have synthesized iodobenzyl-pyro-silane (IPS), a precursor for ORMOSIL with the linked photosensitizer iodobenzylpyropheophorbide (IP). Then, highly monodispersed aqueous dispersion of ORMOSIL nanoparticles, with covalently linked IP, was synthesized upon coprecipitation of IPS with the commonly used ORMOSIL precursor vinyltriethoxysilane (VTES) in the nonpolar core of Tween-80/water microsmulsion. Photophysical studies have demonstrated that the spectroscopic and functional (generation of cytotoxic singlet oxygen) properties of IP are preserved in their "nanoconjugated" state. In vitro experiments have revealed that these nanoparticles are avidly uptaken by tumor cells and show cellular phototoxicity under irradiation with light, thus demonstrating the potential for using them as drug carriers in PDT.

Materials. ORMOSIL precursor vinyltriethoxysilane (VTES) and MTT [3-(4,5-dimethylthiazol-2-yl)-2,5-diphenyltetrazolium bromide] are products of Sigma-Aldrich. Microfuge membrane filters (NANOSEP 100K OMEGA) are a product of Pall Corporation. *N*-Ethyl-*N*′-(3-dimethylaminopropyl) carbodiimide hydrochloride, 4-dimethylamino pyridine, and 4-(triethoxysilyl)-aniline were purchased from Aldrich and used without further purification. 9,10-Anthracenedipropionic acid, disodium salt (ADPA) was purchased from Invitrogen. The Colon-26 and RIF-1 cell lines were obtained from American Type Culture Collection and PDT Center, Roswell Park Cancer Institute, Buffalo. Cells were cultured according to instructions supplied by the vendor. Unless otherwise mentioned, all cell culture products were obtained from Invitrogen.

Synthesis of Iodobenzyl-pyro-silane (IPS). The synthesis of IPS is shown in Scheme 1. First, 3-iodobenzyl-pyro (Compound **I**, 50.0 mg, 0.065 mmol) was taken in a dry round-bottom flask (100 mL) and dissolved in dry dichloromethane (30 mL). To this, 4-(triethoxysilyl)-aniline (19.9 mg, 0.078 mmol), *N*-ethyl-*N*′-(3-dimethylaminopropyl) carbodiimide hydrochloride (24.9 mg, 0.13 mmol), and 4-dimethylamino pyridine (15.8 mg, 0.13 mmol) were added and the resultant mixture was stirred for 14 h at room temperature under N_2 atmosphere. Reaction mixture was then diluted with dichloromethane (100 mL) and washed with brine (50 mL). Then, the organic layer was separated, dried over sodium sulfate, and concentrated. Finally, the product (IPS, Compound **II**) was purified over a silica gel plate using 2.5% methanol−dichloromethane as the mobile phase. Yield: 35.0 mg (53.4%).

NMR spectra were recorded on a Bruker DRX 400 MHz spectrometer at 303 K in $CDCl_3$ solution and referenced to residual $CHCl_3$ (7.26 ppm). ^{1}HNMR (400 Mhz, $CDCl_3$): δ 9.80 (splitted singlet, 1H, meso-H), 8.78 (splitted singlet, 1H, meso-H), 8.55 (splitted singlet, 1H, meso-H), 7.81 (d, 1H, Ar−H, J = 17.6 Hz), 7.65 (t, 1H, Ar−H, J = 8.0 Hz), 7.57 (m, 1H, Ar−H), 7.50 (m, 2H, Ar−H), 7.34−7.29 (m, 3H, Ar−H), 7.08 (m, 1H, Ar−H), 6.00 (m, 1H, CH_3CHOAr), 5.34 (d, 1H, 15^1-CH_2, J = 19.6 Hz), 5.10 (d, 1H, 15^1-CH_2, J = 19.6 Hz), 4.72 (m, 1H, H-17), 4.59 (m, 2H, OCH_2−Ar), 4.41 (m, 1H, H-18), 3.83 (q, 6H, SiOCH_2−CH_3, J = 7.2 Hz), 3.55 (m, 1H, 8-CH_2CH_3), 3.37 (m, 1H, 8-CH_2CH_3), 3.34 (splitted singlet, 3H, ring−CH_3), 3.24 (splitted singlet, 3H, ring-CH_3), 2.81 (m, 1H, 17^2-CH_2), 2.72 (m, 1H, 17^2-CH_2), 2.66 (splitted singlet, 3H, ring−CH_3), 2.36 (m, 1H, 17^1-CH_2), 2.24 (m, 1H, 17^1-CH_2), 2.21 (m, 3H,

Table 1. Formulations of the IPS Nanoparticles

name	IPS (10 mM):VTES (4.8 M) vol ratio	IPS:VTES absolute molarity (μM:mM)	IPS:VTES molar ratio
NY-362	1:0	40:0	1:0
NY-363	1:1	40:19.2	1:480
NY-364	1:2	40:38.4	1:960
NY-365	1:4	40:76.8	1:1920

CH_3CH−OAr), 1.81 (d, 3H, 18-CH_3, J = 7.2 Hz), 1.53 (m, 3H, 8-CH_2CH_3), 1.20 (t, 9H, $SiOCH_2-CH_3$, J = 6.8 Hz), 0.45 (brs, 1H, NH), −1.53 (brs, 1H, NH). EIMS: 1007 ($M^+ + 1$).

Synthesis and Characterization of the Covalently Linked Iodobenzylether-pyro Nanoparticles. In general, the nanoparticles were synthesized by the alkaline hydrolysis and polycondensation of the organotrialkoxysilane precursors within the nonpolar core of Tween-80/water microemulsion. Briefly, to 10 mL of 2% aqueous Tween-80 solution, 300 μL of co-surfactant 1-butanol was dissolved. To this solution, 40 μL of a solution (10 mM in DMSO) of IPS (Compound **II**, Scheme 1) was dissolved by simple magnetic stirring. Next, 0 or 40 or 80 or 160 μL of VTES was added dropwise, and the resulting mixture was magnetically stirred for 1 h. At this stage, 10μL of aqueous ammonia was added and the resulting solution was magnetically stirred overnight, leading to the formation of the nanoparticles. To study the difference between conjugated and encapsulated PS in ORMOSIL, we also synthesized PS encapsulated nanoparticles by an identical procedure as described above, except that 40 μL of 10 mM DMSO solution of IP (Compound **I**, Scheme 1) was used instead of IPS. Next, the nanoparticles were dialyzed overnight against distilled water using a cellulose membrane of cutoff pore size of 12−14 kD for the removal of unreacted molecules. The dialysate containing the IP-conjugated ORMOSIL nanoparticles was sterile-filtered (0.2 uM membrane) and was stored at 4 °C for further use. Table 1 represents the amounts of the IPS and VTES used in the various formulations.

To separate the Tween-80 micelles (and any associated free PS) from the nanoparticles, the dialyzed dispersions were filtered in a microfuge membrane filter (NANOSEP 100K OMEGA, Pall Corporation) by centrifuging at 14 000 rpm for 30 min (spin-filtration). Tween-80 micelles and their associated free PS molecules flowed through this membrane and are collected in the lower tube (fliltrate), while nanoparticles got embedded in the membrane and could be subsequently extracted by adding water and sonicating/vortexing briefly (retentate). The amount of PS associated with each fraction could be estimated by reading their optical density at 663 nm (the long wavelength absorption peak for IP/IPS). All subsequent studies with the nanoparticles were carried out with the micelle-free "retentate" fraction unless otherwise mentioned.

Thin-layer chromatography (TLC) was done on ANALTECH precoated silica gel GF PE sheets (cat. 159017, layer thickness 0.25 mm). Preparative TLC plates were used for the purification (ANALTECH precoated silica gel GF glass plate, cat. 02013, layer thickness 1.0 mm). Dichloromethane was dried over P_2O_5 under N_2 atmosphere.

Characterization of Size, Shape, and Functionality of the Nanoparticles. Transmission electron microscopy (TEM) was performed to determine the size and shape of the prepared nanoparticles by using a JEOL JEM-100cx microscope at an accelerating voltage of 80 kV. UV−visible absorption spectra were acquired by using a Shimadzu UV-3600 spectrophotometer in a quartz cuvette with 1 cm path length. Fluorescence spectra were recorded on a Fluorolog-3 spectrofluorometer (Jobin Yvon, Longjumeau, France). Generation of singlet oxygen ($^1O_2$) was detected by its phosphorescence emission peaked at 1270 nm.[11−13] A SPEX 270M Spectrometer (Jobin Yvon) equipped with a Hamamatsu IR-PMT was used for recording singlet oxygen phosphorescence spectra. The sample solution in a quartz cuvette was placed directly in front of the entrance slit of the spectrometer, and the emission signal was collected at 90° relative to the exciting laser beam. A 514 nm laser line from Argon ion laser (Spectra-Physics) was used for excitation. Additional long-pass filters (a 950LP filter and a 538AELP filter, both from Omega Optical) were used to attenuate the scattered light and fluorescence from the samples.

$^1O_2$ phosphorescence decays at 1270 nm were acquired using Infinium oscilloscope (Hewlett-Packard) coupled to the output of the PMT. A second harmonic (532 nm) from a nanosecond pulsed Nd:YAG laser (Lotis TII, Belarus) operating at 20 Hz was used as the excitation source in this case.

Chemical oxidation of ADPA in the aqueous suspension of the nanoparticles was used as an independent method to characterize singlet oxygen generation efficiency.[11,14,15] In this case, a decrease in the absorbance of the ADPA added to the aqueous suspensions of the nanoparticles was monitored as a function of time, following irradiation with 514 nm laser light.

In Vitro Studies with Tumor Cells: Nanoparticle Uptake and Imaging. For studying nanoparticles uptake and imaging, Colon-26 cells were used, maintained in RPMI-1640 media with 10% fetal bovine serum (FBS) and appropriate antibiotic. The cells at a confluency of 70−75% were treated overnight with the nanoparticles at a final photosensitizer concentration of 2 μM. The next day, the treated cells were washed thoroughly with PBS and then directly imaged using a confocal laser scanning microscope (MRC-1024, Bio-Rad, Richmond, CA). A water immersion objective lens (Nikon, Fluor-60X, NA = 1.0) was used for cell imaging. A Ti:sapphire laser (Tsunami from Spectra-Physics) pumped by a diode-pumped solid-state laser (Millenia, Spectra-Physics) was used as a source of excitation. The Ti:sapphire output, tuned to 830 nm, was frequency doubled by second harmonic generation (SHG) in a β-barium borate (β-BBO) crystal to obtain the 415 nm light, and was coupled into a single mode fiber for delivery into the confocal scan head. A long-pass filter, 585 LP (585 nm), and an additional band-pass filter with transmission at 680 ± 15 nm (Chroma 680/30) were used as emission filters for fluorescence imaging.

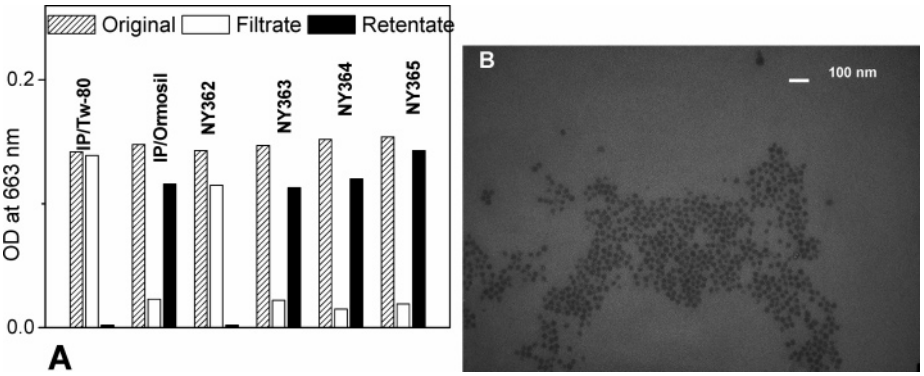

Figure 1. (A) Results of spin-filtration of various formulations of PS/nanoparticles and (B) TEM image of NY-363.

In Vitro PDT. The RIF-1 tumor cells, grown in α-minimum essential medium (α-MEM) with 10% fetal calf serum, L-glutamine, and penicillin/streptomycin/neomycin, were maintained in 5% CO2, 95% air, and 100% humidity. These cells were plated in 96-well plates at a density of 5×10^3 cells/well in complete medium as a means to determine PDT efficacy. The next day, the IPS-conjugated nanoparticles were added at a concentration corresponding to 0.5 μM of IP. After the 24 h incubation in the dark at 37 °C, the cells were replaced with fresh media and exposed to light at a dose rate of 3.2 mW/cm^2 at various light doses (0.125−8.0 J). The dye laser (375; Spectra-Physics, Mountain View, CA) excited by an argon-ion laser (171 laser; Spectra-Physics, Mountain View, CA) was tuned to emit at the drug-activating wavelength of 665 nm. Uniform illumination was accomplished by using a 600 μm diameter quartz optical fiber fitted with a graded index refraction lens. Following illumination, the plates were incubated at 37 °C in the dark for 48 h. Appropriate control experiments using identical light doses without any photosensitizer were also performed. After this, the plates were evaluated for cell viability using the MTT assay as described below.

Cell Viability Assay. Cell viability was measured using the 3-[4,5-dimethylthiazol-2-yl]-2,5-diphenyl tetrazolium-bromide (MTT) assay.[11,17] Immediately following light treatment, the cells were incubated for 44 h in the dark at 37 °C. Then, 10 μL of 4.0 mg/mL solution of MTT dissolved in PBS was added to each well. After 4 h incubation with the MTT, the media were removed and 100 μL of dimethyl sulfoxide was added to solubilize the formazin crystals. The PDT efficacy was measured by reading the 96-well plate on a microtiter plate reader (Miles Inc., Titertek Multiscan Plus MK II) at an absorbance of 560 nm. The results were plotted as percent survival compared with the corresponding control experiments results (cells were not incubated with drug, but exposed to light). Each data point represents the mean from a typical experiment with six replicate wells.

Results and Discussions. Figure 1A shows the relative optical densities (read at 663 nm, the long-wavelength absorbance peak for IP) of the "filtrate" and "retentate" fractions, as well as the nonfiltered "original" samples, for NY-362 through NY-365. The non-silylated photosensitizer 3-iodobenzyl-pyro, or IP (compound **I**, Scheme 1), was used as the control, dissolved in Tween-80 micelles as well as encapsulated in ORMOSIL nanoparticles.

From Figure 1A, it is evident that while NY-362 does not form any nanoparticles and most of the IPS is associated with the Tween-80 micelles that are collected in the filtrate, almost 80−90% of the IPS is associated with the nanoparticles in NY-363 through NY-365, which can be collected as the "retentate". Inability of pure IPS to form the nanoparticles is evidently associated with the steric hindrances due to bulky IP moieties, and nanoparticles are formed by combining both IPS and VTES precursors. A formation of the rigid, spherical, and monodisperse nanoparticles with size about 20 nm is shown by TEM for NY-363 (Figure 1B). It is worth noting that, while TEM of NY-362 showed no formation of nanoparticles, thus confirming the inability of IPS alone to form nanoparticles, NY-364 and NY-365 both formed the same-sized nanoparticles as NY-363 (data not shown), showing that the size of the nanoparticles is unaffected by the amount of the precursor used. Because the size of the nanoparticles and the amount of IPS remain the same upon increasing the amount of VTES (see Table 1), the overall number of the nanoparticles are increasing in the order NY-363 < NY-364 < NY-365, and the number of IP moieties per nanoparticle are getting diluted in the order NY-363 > NY-364 > NY-365. To confirm that IP is conjugated with the nanoparticles, and not merely physically associated, we have run both IP-conjugated and IP-encapsulated nanoparticles as well as IP/micelles on silica-thin layer chromatography (silica-TLC) plates in organic media (ref ∼ 0.5 in 10% methanol−dichloromethane) (Figure 2). It can be seen that, while the IP encapsulated in the nanoparticles (lane 2) runs similar to IP in Tween-80 micelles (lane 3) in the direction of the solvent front, the IP conjugated with the nanoparticles (NY-363) remains at the bottom, along with the nanoparticles (lane 1). This means that the organic medium is not able to wash away the IP molecules from the NY-363, indicating covalent linkage. We obtained similar data for NY-364 and NY-365 (data not shown). In sharp contrast, encapsulated IP molecules can be easily extracted from the nanoparticles by organic solvents, as seen in the TLC plate (lane 2), similarly to results obtained for IP in Tween-80 micelles (lane 3).

Absorption and fluorescence of the IP covalently incorporated into nanoparticle matrix are similar to that of

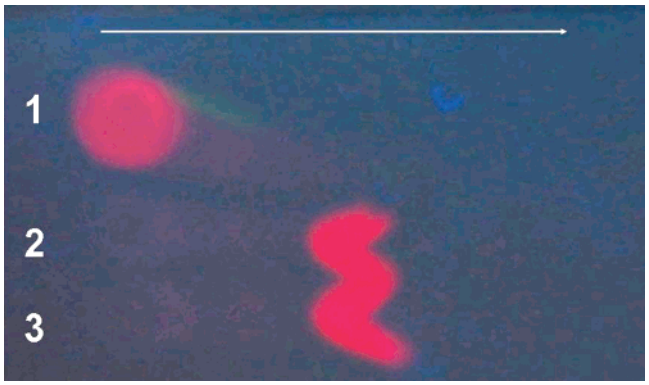

Figure 2. Emission of IP upon UV irradiation following TLC of IP-conjugated (lane 1) and encapsulated (lane 2) ORMOSIL nanoparticles. Lane 3 shows the same for IP/1% Tween-80.

encapsulated in the Tween-80 micelles (Figure 3). While samples of NY-363, NY-364, and NY-365 have almost identical absorption and fluorescence spectra, NY-362 (nonspin-filtered) shows some decrease in the fluorescence intensity. This correlates with slight broadening of long-wave absorption band and can originate from the interaction of the IPS chromophores in Tween-80 micelles (self-aggregation).

Aggregation of the PS chromophores is usually manifested both in a decrease of fluorescence intensity and singlet oxygen generation.[16,17] Figure 4A presents emission spectra of singlet oxygen sensitized by samples of suspensions with absorbance and fluorescence shown in Figure 3. Because of the extremely low yield of singlet oxygen phosphorescence in water,[18] we have used methanol solution of Rose Bengal as a standard. As seen in Figure 4A, IP chromophores incorporated within nanoparticles are capable of generating singlet oxygen with a yield comparable to that of $^1O_2$ generated by IP/Tween-80 micelles. Intensity of the singlet oxygen emission sensitized in all suspensions of nanoparticles/micelles correlates with fluorescence intensity (Figure 3B). Intensity of $^1O_2$ emission as well as fluorescence is almost identical for NY-363, NY-364, and NY-365. IP/Tween-80 micellar suspension shows slightly higher fluorescence and $^1O_2$ emission intensities, whereas the intensity for NY-362 (nonspin-filtered) is lower. It should be noted that Figure 4A shows raw spectra, including background, and $^1O_2$ emission relative intensity can be estimated with the background subtraction. Correlation of the fluorescence and $^1O_2$ emission intensities confirms aggregation affecting singlet oxygen generation. It is worth noting that the amount of singlet oxygen generated by PS (IP) in surfactant (Tween-80) micelles does depend on the relative amount of surfactant, which protects hydrophobic PS molecules from aggregation. Absence of any difference in absorption/fluorescence/singlet oxygen generation for the samples NY-363, NY-364, and NY-365 shows that the aggregation effect does not manifest itself in the micelle-free IPS/VTES nanoparticles and relative content of IPS within nanoparticles can be further increased to obtain higher $^1O_2$ generation for more efficient PDT action.

Singlet oxygen phosphorescence steady-state spectroscopy well characterizes singlet oxygen generation in a homogeneous medium. However, in a heterogeneous medium (i.e., aqueous dispersion of the nanoparticles with embedded photosensitizer), a question arises how the observed $^1O_2$ phosphorescence intensity will correlate with phototoxic efficiency of the generated $^1O_2$ because it could be, in principle, mostly deactivated within nanoparticles due to the limited lifetime of $^1O_2$. We have used singlet oxygen mediated bleaching of the ADPA as an independent method for investigating the functional effect of the generated $^1O_2$ outside nanoparticles. Here, we have added ADPA to the suspension of nanoparticles and recorded the time-dependent reduction of the ADPA absorption peak at 400 nm upon continuous irradiation with laser light (514 nm). The slope of the curves obtained is an indication of the functional efficiency of generated singlet oxygen (more the slope, more is the efficiency).[14] As seen in Figure 4B, results on singlet oxygen production, which were obtained with the method of ADPA bleaching, showed a remarkable similarity to those obtained by singlet oxygen phosphorescence spectroscopy (Figure 4A) by following the same trend: IP/Tween-80 micellar suspension demonstrated higher $^1O_2$ generation than NY-363, NY-364, and NY-365, whereas the intensity for NY-362 is lower. This means that singlet oxygen generated within nanoparticles is mostly deactivated outside nanoparticles, causing bleaching of ADPA. In this case, the lifetime of the singlet oxygen generated within the nanoparticles should be determined by the water environment. Figure 5 shows decays of the detector response at 1270 nm for the IPS/VTES nanoparticle and IP/Tween-80 suspensions. Along with a fast decay component coming from the scattered excitation light, one can see a slow component with characteristic lifetime in the microsecond range, which is definitely from the singlet oxygen phosphorescence decay. Decays of $^1O_2$ emission sensitized by IPS/VTES are very close to that sensitized by IP/Tween-80 micellar suspension and have average lifetime (τ) in the range of 4.5−5 μs. In Figure 5, decay of $^1O_2$ emisssion sensitized by RB in methanol is also shown, demonstrating monoexponential fitting with $\tau \approx 10$ μs, which is the characteristic lifetime for $^1O_2$ in methanol.[18] The rise time of the $^1O_2$ emission sensitized by the nanoparticle/micellar suspensions is noticeably higher than for the RB molecular solution, including the time of diffusion of molecular oxygen to the incorporated PS chromophores. However, because decay time is close enough to that for $^1O_2$ in water (4 μs)[19] and the action of the singlet oxygen is demonstrated in the ADPA bleaching experiment, we consider that IP chromophores within the IPS/VTES nanoparticles retain their functionality as PS for PDT.

Because the nanoparticles are capable of singlet oxygen production, which is an indispensable condition for successful application in PDT, we tested cellular uptake of the nanoparticles in vitro. Figure 6 presents confocal images of Colon-26 cells treated overnight with the nanoparticles of NY-363, NY-364, and NY-365 formulation. As one can see, there is a significant uptake of the nanoparticles for all formulations. Because imaging conditions were maintained the same (in particular, confocal pinhole and aperture for fluorescence

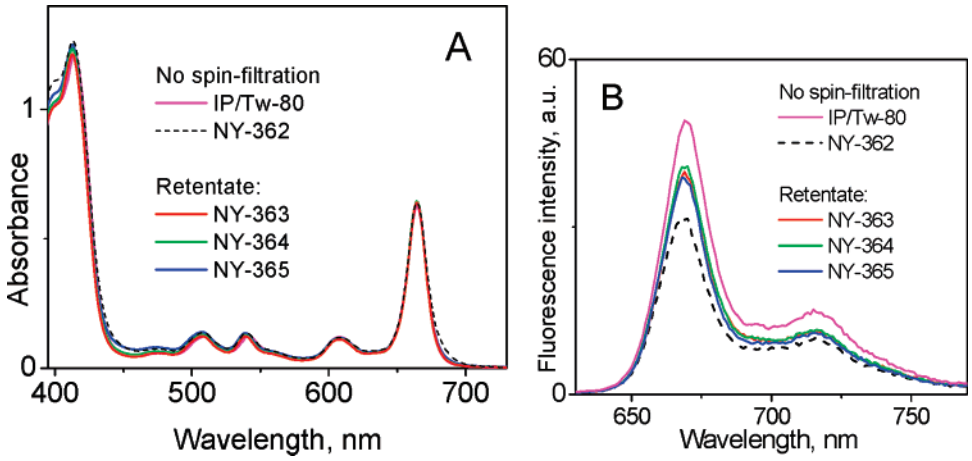

Figure 3. Absorption (A) and fluorescence (B) spectra of the "spin-filtered" nanoparticle samples (retentate collected after spin-filtration and resuspended in water), as well as nonfiltered micellar suspensions of IP/Tween-80 and NY-362 (100% of IPS, no VTES). Fluorescence was excited with 514 nm.

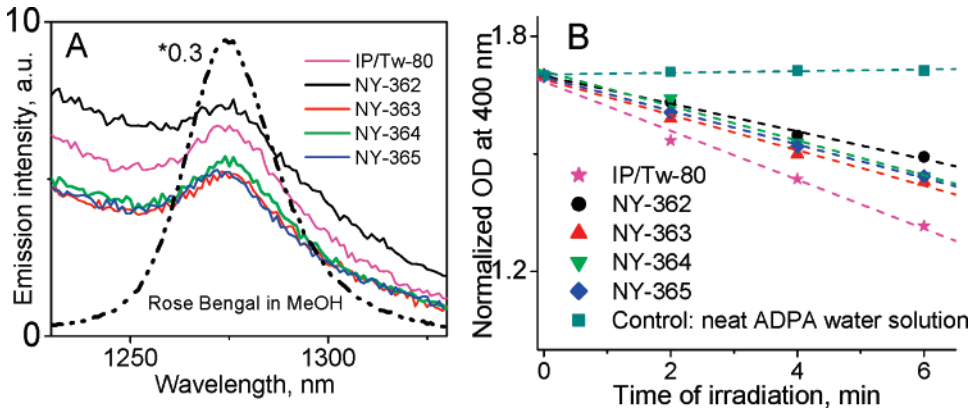

Figure 4. Determination of singlet oxygen generation efficiency for the "micelle-free" suspensions of nanoparticles. Nonspin-filtered micellar suspensions of IP/Tween-80 and NY-362 (100% of IPS, no VTES) were used as controls. Rose Bengal (RB) in methanol was used as the reference standard for the $^1O_2$ phosphorescence measurements. Irradiation with 514 nm, laser beam power was 150 mW for the bleaching experiment and 30 mW for spectra acquisition.

imaging), one can see that fluorescence intensity for NY-364 is higher than for NY-365 and is the highest for NY-363. It corresponds to the amount of the IP moieties (N) within nanoparticles ($N_{NY363} > N_{NY364} > N_{NY365}$). This is understandable, assuming that the average amount of the nanoparticles uptaken by the cells is similar for all formulations.

To check whether uptaken nanoparticles are capable of photodynamic effect, we have performed study of the in vitro photosensitizing activity for different nanoparticle formulations. As shown in the Figure 7, the nanoparticles manifest phototoxic effect on the cultured cells and it is proportional to the irradiating light dose. Moreover, phototoxicity of the nanoparticles is proportional to the cellular uptake, as it follows from the comparison of Figures 6 and 7. These data support our assumption that the average amount of the nanoparticles uptaken by the cells is similar for all formulations, and the highest photodynamic effect produced by NY-363 is associated with the highest content of the IP chromophore within the nanoparticle.

Conclusions. Synthesis of highly monodispersed aqueous dispersion of ORMOSIL nanoparticles with covalently

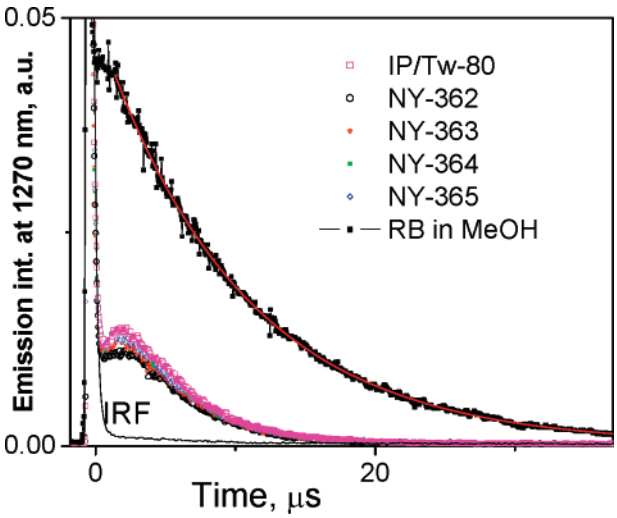

Figure 5. Decays of the detector response at 1270 nm for the IPS/VTES nanoparticle and IP/Tween-80 suspensions. Signal obtained for the suspension of neat ORMOSIL nanoparticles (100% of VTES) was used as instrument response function (IRF). Rose Bengal (RB) in methanol was used as reference standard producing singlet oxygen.

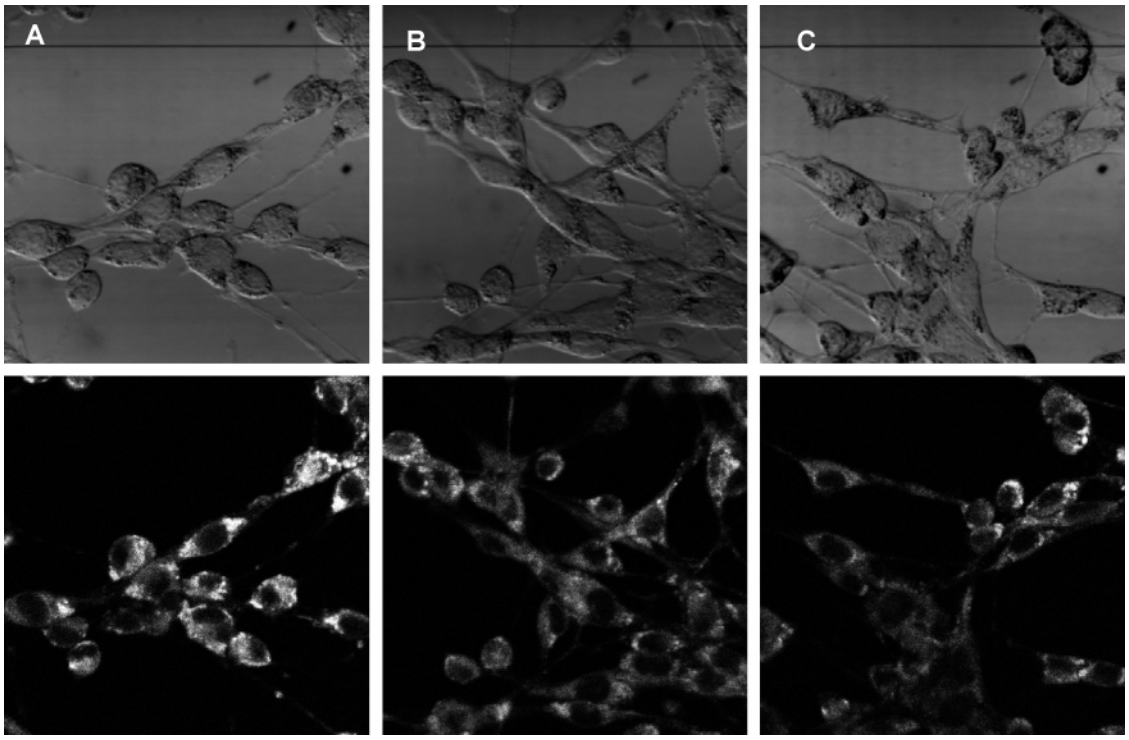

Figure 6. Colon-26 cells treated overnight with NY-363 (A), NY-364 (B), NY-365 (C). Transmission (above) and fluorescence (below) channels are shown. Confocal pinhole and PMT gain remained same during imaging.

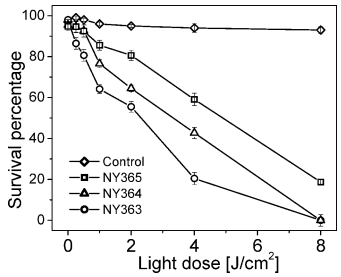

Figure 7. Comparative in vitro photosensitizing efficacy of nanoparticle formulations. RIF-1 cells were treated with nanoparticles to have same concentration of IP in every well (0.5 μM). Control: Cells were exposed to light without photosensitizer.

incorporated PS molecule is reported. Photophysical characterization has shown that the spectroscopic and functional (generation of cytotoxic singlet oxygen) properties of the PS moieties are preserved in their "nanoconjugated" state. These nanoparticles are also avidly taken up by tumor cells in culture and show phototoxicity in treated cells upon irradiation with light, thus demonstrating the potential of these nanoparticles for PDT. In addition, it is also possible to chemically replace the iodine atom of the iodinated photosensitizer (IP) with a radiolabeled iodine atom (e.g., I-124, I-125, etc.), thus converting these nanoparticles as contrast agents for PET/SPECT imaging while preserving their therapeutic functionality. We have already demonstrated using non-nanoparticulate formulations that such bifunctional agents can be used for both diagnosis and PDT of cancer, using a "see-and-treat" approach.[20] Studies are underway to render "multimodality" to these nanoparticles by additionally incorporating diagnostic agents as well as biotargeting molecules following suitable surface functionalization.[21−23]

Acknowledgment. This work was supported by grants form the National Institutes of Health (R01CA119358-01, and RO1CA104492) and the John R. Oishei Foundation. We thank Jessica R. Zinaty and Lisa A. Vathy for their technical support.

References

(1) Dougherty, T. J. *Photochem. Photobiol.* **1987**, *45*, 879.
(2) Chen, B.; Pogue, B. W.; Hoopes, P. J.; Hasan, T. *Crit. Rev. Eukaryotic Gene Expression* **2006**, *16*, 279.
(3) Konan, Y. N.; Gruny, R.; Allemann, E. *J. Photochem. Photobiol. B* **2002**, 66, 89.
(4) Taillefer, J.; Jones, M. C.; Brasseur, N.; Van Lier, J. E.; Leroux, J. C. *J. Pharm. Sci.* **2000**, *89*, 52.
(5) van Nostrum, C. F. *Adv. Drug Delivery Rev.* **2004**, *56*, 9.
(6) Wang, S.; Gao, R.; Zhou, F.; Selke, M. *J. Mater. Chem.* **2004**, *14*, 487.
(7) Gao, D.; Agayan, R. R.; Xu, H.; Philbert, M. A.; Kopelman, R. *Nano Lett.* **2006**, *6*, 2383.
(8) Maeda, H.; Wu, J.; Sawa, T.; Matsumura, Y.; Hori, K. *J. Controlled Release* **2000**, *65*, 271.
(9) Prasad, P. N. *Introduction to Biophotonics*; Wiley-Interscience: New York, 2004.
(10) Hasan, T. *Photodynamic Therapy: Basic Principles and Clinical Applications*; Mercel Dekker: New York, 1992.
(11) Roy, I.; Ohulchanskyy, T. Y.; Pudavar, H. E.; Bergey, J. E.; Oseroff, A. R.; Morgan, J.; Dougherty, T. J.; Prasad, P. N. *J. Am. Chem. Soc.* **2003**, *125*, 7860.
(12) Frederiksen, P. K.; Jorgensen, M.; Ogilby, P. R. *J. Am. Chem. Soc.* **2001**, *123*, 1215.
(13) Ohulchanskyy, T. Y.; Donnelly, D. J.; Detty, M. R.; Prasad, P. N. *J. Phys. Chem. B* **2004**, *108*, 8668.
(14) Lindig, B. A.; Rodgers, M. A. J.; Schaap, A. P. *J. Am. Chem. Soc.* **1980**, *102*, 5590.
(15) Kim, S.; Ohulchanskyy, T. Y.; Pudavar, H. E.; Pandey, R. K.; Prasad, P. N. *J. Am. Chem. Soc.* **2007**, *129*, 2669.
(16) Zenkevich, E.; Sagun, E.; Knyukshto, V.; Shulga, A.; Mironov, A.; Efremova, O.; Bonnett, R.; Songca, S. P.; Kassem, M. *J. Photochem. Photobiol. B* **1996**, *33*, 171.

(17) Rosenfeld, A.; Morgan, J.; Goswami, L. N.; Ohulchanskyy, T.; Zheng, X.; Prasad, P. N.; Oseroff, A.; Pandey, R. K. *Photochem. Photobiol.* **2006**, *82*, 626.
(18) Losev, A. P.; Byteva, I. M.; Gurinovich, G. P. *Chem. Phys. Lett.* **1988**, *143*, 127.
(19) Chou, P.-T.; Khan, S.; Frei, H. *Chem. Phys. Lett.* **1986**, *129*, 463.
(20) Pandey, S. K.; Gryshuk, A. L.; Sajjad, M.; Zheng, X.; Chen, Y.; Abouzeid, M. M.; Morgan, J.; Charamisinau, I.; Nabi, H. A.; Oseroff, A.; Pandey, R. K. *J. Med. Chem.* **2005**, *48*, 6286.
(21) Roy, I.; Ohulchanskyy, T. Y.; Bharali, D. J.; Pudavar, H. E.; Mistretta, R. A.; Kaur, N.; Prasad, P. N. *Proc. Natl. Acad. Sci.U.S.A.* **2005**, *102*, 279.
(22) Bharali, D. J.; Lucey, D. W.; Jayakumar, H.; Pudavar, H. E.; Prasad, P. N. *J. Am. Chem. Soc.* **2005**, *127*, 11364.
(23) Qian, J.; Yong, K.-T.; Roy, I.; Ohulchanskyy, T. Y.; Bergey, E. J.; Lee, H. H.; Tramposch, K. M.; He, S.; Maitra, A.; Prasad, P. N. *J. Phys. Chem. B* **2007**, *111*, 6969.

NL0714637